Cutting Edge

The Journal of Immunology

Cutting Edge: The Heat Shock Protein gp96 Activates Inflammasome-Signaling Platforms in APCs

Yifei Wang,*,† Abigail L. Sedlacek,† Sudesh Pawaria,‡ Haiyan Xu,§ Melanie J. Scott,¶ and Robert J. Binder†

Several heat shock proteins (HSPs) prime immune responses, which are, in part, a result of activation of APCs. APCs respond to these immunogenic HSPs by upregulating costimulatory molecules and secreting cytokines, including IL-1β. These HSP-mediated responses are central mediators in pathological conditions ranging from cancer, sterile inflammation associated with trauma, and rheumatoid arthritis. We tested in this study the requirement of inflammasomes in the release of IL-1β by one immunogenic HSP, gp96. Our results show that murine APCs activate NLRP3 inflammasomes in response to gp96 by K^+ efflux. This is shown to initiate inflammatory conditions in vivo in the absence of additional known inflammasome activators or infection. These results document a novel mechanism by which proteins of endogenous origin, the HSPs, can modulate an inflammatory response following their release from aberrant cells. *The Journal of Immunology*, **2018, 201: 2209–2214.**

Immunization of mice and humans with select heat shock proteins (HSPs) initiates a program of inflammation characterized by the release of IL-1β, IL-6, and TNF-α from APCs (1, 2). These cytokines are partially responsible for eliciting Th1 responses (1); the other components being upregulation of costimulation by the APC (2) and cross-presentation of HSP-chaperoned peptides (3). Although there has been a great interest in harnessing these Th1 responses for the immunotherapy of cancer and infectious disease (4), the complexities of cytokine release by APCs have not yet been fully investigated. Importantly, the distinct signaling pathways and final repertoire of cytokines released is dependent on the APC that is engaged by the HSP (1, 2, 5, 6) and the contribution of other signals in the microenvironment (1). These mechanisms allow HSPs to prime Th1 (3), Th17 (1), or regulatory T cell responses (6, 7). The release of IL-1β from a variety of APCs, including dendritic cells (DCs) and macrophages, in response to HSPs, has conspicuously lacked a basic characterization even though this seminal observation was made over 17 y ago (2). Although the predominant mechanism for IL-1β maturation and release from cells requires the activation of inflammasomes (8), several inflammasome-independent pathways have been described (9).

The inflammasome is a central component of the innate immune system geared toward recognizing changes in cellular homeostasis and generating responses for clearing pathogens and for tissue repair. As a multimeric protein complex, it is responsible for activation of caspase-1, which proceeds to cleave multiple substrates, including pro–IL-1β and pro–IL-18, into their mature form (8).

We show that the prototypical immunogenic HSP, gp96, initiates two signals in APCs: 1) an NF-κB and p38-dependent upregulation in the synthesis of pro–IL-1β, and 2) activation of the NLRP3 inflammasome itself. The release of HSPs into the extracellular environment, in the absence of obvious infection or pathogens, is a molecular trigger for inflammation and is relevant for conditions ranging from sterile inflammation, rheumatoid arthritis, and cancer-associated inflammation.

Materials and Methods

Mice

Wild type (WT) C57BL/6 mice from The Jackson Laboratory (Bar Harbor, ME) were housed in the animal facility Division of Laboratory Animal Resources at the University of Pittsburgh. $CD91^{fl/fl}CD11c^{cre}$ mice have been previously described (10). $NLRP3^{-/-}$ mice were a gift from Dr. T. Billiar (University of Pittsburgh). Gasdermin D (GD)–deficient mice ($GD^{-/-}$) were obtained from Dr. V. Dixit (11) (Genentech, CA) and bred in-house.

*School of Medicine, Tsinghua University, Beijing 100084, China; †Department of Immunology, University of Pittsburgh, Pittsburgh, PA 15261; ‡Department of Medicine, University of Massachusetts Medical Center, Worcester, MA 01655; §Department of Urology, Third Affiliated Hospital of Soochow University, Changzhou, 213003 Jiangsu, China; and ¶Department of Surgery, University of Pittsburgh, Pittsburgh, PA 15261

ORCIDs: 0000-0001-8890-6859 (Y.W.); 0000-0001-5623-6723 (A.L.S.); 0000-0003-0948-5238 (H.X.).

Received for publication April 13, 2018. Accepted for publication August 16, 2018.

This work was supported by National Institutes of Health (NIH) Grant CA208833 (to R.J.B.), University of Pittsburgh Immunology Department start-up funds (to R.J.B.), and NIH Grant R01-GM-102146 (to M.J.S.). This work benefitted from IMAGESTREAMX MARKII funded by NIH Grant 1S10OD019942-01 (L. Borghesi, principal investigator). Tsinghua University School of Medicine provided funds (to Y.W.) through a collaborative education and research agreement with the University of Pittsburgh.

Address correspondence and reprint requests to Dr. Robert J. Binder, University of Pittsburgh, E1058 Biomedical Science Tower, 200 Lothrop Street, Pittsburgh, PA 15261. E-mail address: rjb42@pitt.edu

The online version of this article contains supplemental material.

Abbreviations used in this article: DAMP, damage-associated molecular pattern; DC, dendritic cell; GD, gasdermin D; HSP, heat shock protein; PEC, peritoneal exudate cell; ROS, reactive oxygen species; WT, wild type.

Cell culture

Peritoneal exudate cells (PECs) were collected from the peritoneal cavity of mice with PBS and cultured overnight in RPMI 1640 complete medium (5% FBS) to obtain the adherent population. DCs were differentiated from mouse bone marrow cells for 6 d with 0.02 μg/ml GM-CSF (added on days 0 and 3). B16 (containing empty plasmid) and B16/gp96 cells were cultured in complete DMEM medium (10% FBS) with 0.4 g/l G418.

Reagents and inhibitors

Gp96 was purified from mouse livers and verified by SDS-PAGE and immunoblotting (2). Endotoxin contamination is determined to be below the detection limit of the *Limulus* amebocyte lysate (2). One nanogram of LPS (Sigma-Aldrich) is equivalent to 5 endotoxin units (*Limulus* amebocyte lysate assay) or 10 endotoxin units (chromogenic assay). Where indicated, PECs were treated with 10 μM of nigericin (Tocris Bioscience), 10 μM of the NF-κB inhibitor cardamonin (Sigma-Aldrich), 15 μM of the p38 MAPK inhibitor SB203580 (Calbiochem), 20 μg/ml caspase-1 inhibitor YVAD (Calbiochem), 2 mM of the reactive oxygen species (ROS) scavenger *N*-acetylcysteine (MP Biomedicals), or 25 μM of the P_2X_7 inhibitor A438079 (Tocris Bioscience). *N*-Acetylcysteine and A438079 were verified to block IL-1β production by PECs treated with LPS plus ATP (data not shown). Treatments started 30 min prior and lasted for the duration of the experiment. Cell lysates were analyzed by SDS-PAGE and immunoblotting with primary and HRP-conjugated secondary Abs. Primary Abs to pro–IL-1β, NLRP3, ASC, and β-Actin were from Cell Signaling Technology, and to caspase-1 (p20) were from AdipoGen Life Sciences. The FLICA assay was performed using FAM FLICA Caspase-1 Kit (Bio-Rad Laboratories). The APC Annexin V Apoptosis Detection Kit (BioLegend) was used for the cell death experiments.

Procedures

ASC oligomerization was performed according to Katsnelson et al. (12). IL-1β was measured by ELISA (Thermo Fisher Scientific). Blood was collected from orbital sinus of mice, and serum was harvested by centrifugation.

Flow cytometry

Mice were injected with 2×10^6 B16 or B16/gp96 cells i.p. After 8 or 18 h, PECs were harvested and fixed/permeabilized (BD Biosciences), followed by staining with Abs; F4/80 (PerCP-Cy5.5), pro–IL-1β (APC), and anti-mouse IgG (FITC) were from eBioscience, CD11b (PE-Cy7) and Ly-6G (PE) from BD Biosciences, and CD91 from Abcam. Data acquisition was performed with BD LSR II or BD LSRFortessa instruments and analyzed using FlowJo. Data acquired by the Amnis ImageStream (ImageStream Mark II) were analyzed with IDEAS 6.2.

Statistical analyses

Statistical analyses were performed with Prism Software using ANOVA or two-tailed *t* test for comparison between two variables. Statistical significance was defined as $^*p < 0.05$, $^{**}p < 0.01$, $^{***}p < 0.001$, and $^{****}p < 0.0001$. Graphs are mean ± SD.

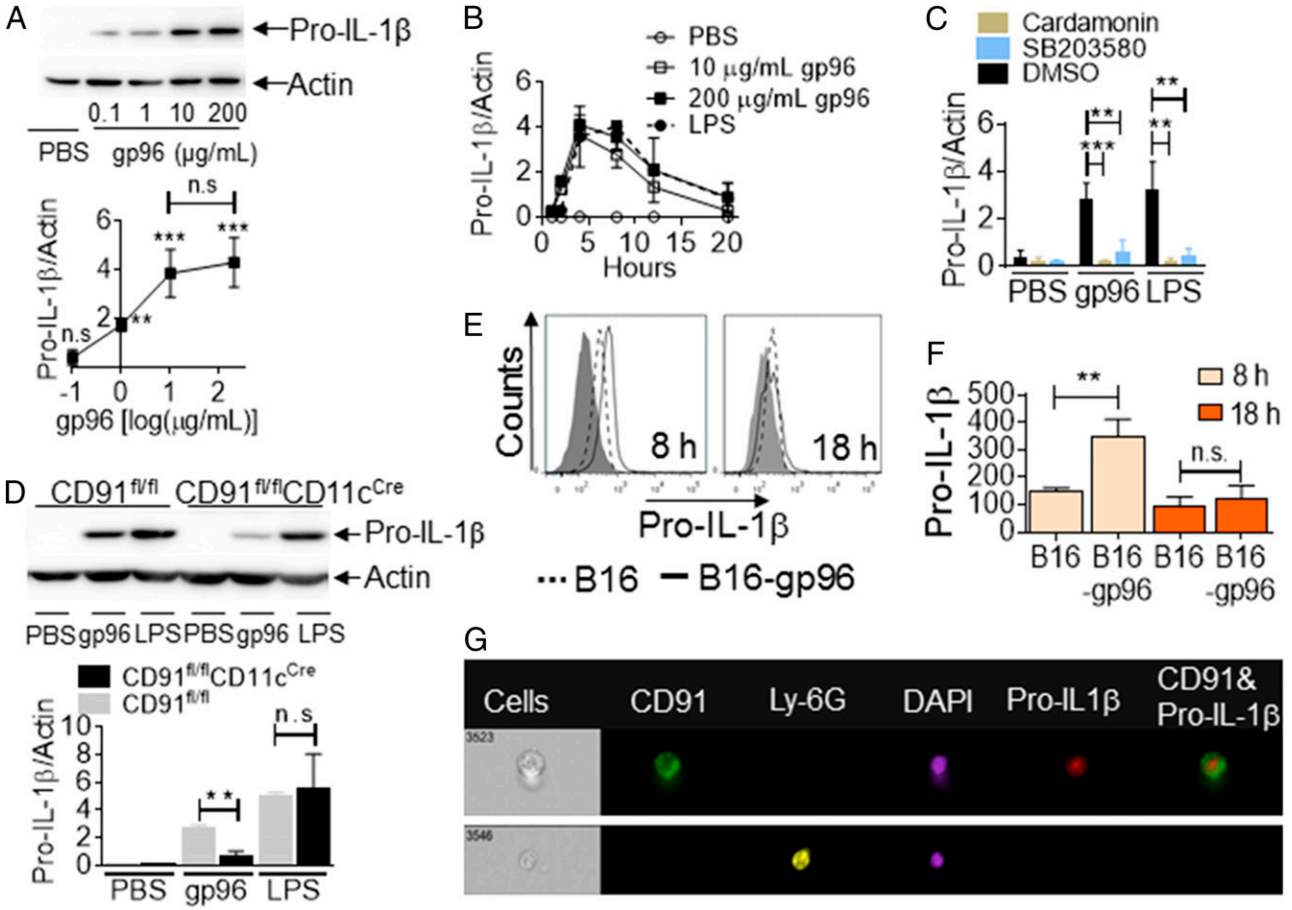

FIGURE 1. Gp96 induces synthesis of pro–IL-1β in a CD91-dependent manner. (**A** and **B**) PECs were treated with gp96 at the indicated concentration or PBS. Cell lysates were analyzed for pro–IL-1β protein by SDS-PAGE and immunoblotting at 4 h (A) or over a time period from 0 to 20 h (B). (**C**) PECs were pretreated with cardamonin, SB203580, or DMSO, followed by incubation with 200 μg/ml gp96 or 10 μg/ml LPS or PBS. Pro–IL-1β protein level was measured as in (A). (**D**) DCs from $CD91^{fl/fl}$ or $CD91^{fl/fl}CD11c^{Cre}$ mice were treated with 200 μg/ml gp96 or 10 μg/ml LPS or PBS for 4 h. Pro–IL-1β was analyzed as in (A). In (A)–(D), the amount of pro–IL-1β was quantified and normalized to actin as a loading control. In (A), comparisons are made to PBS-treated cells. (**E**–**G**) B16 or B16/gp96 cells were implanted into the peritoneal cavity of mice. PECs were harvested after 8 or 18 h and analyzed by flow cytometry with gating on macrophages (F4/80) and CD91 and further on intracellular pro–IL-1β (E). Gray filled histogram is Ab isotype staining. Mean fluorescence intensity (MFI) from the histograms are presented in (F). (G) PECs were further analyzed with markers for neutrophils (Ly6G). Data are from one representative experiment of three to five independent experiments. $^{**}p < 0.01$, $^{***}p < 0.001$.

Results and Discussion

The immunogenic HSP gp96 upregulates expression of pro–IL-1β in macrophages

As a substrate for inflammasome activity, we probed for the expression of pro–IL-1β in murine-isolated, adherent PECs in response to gp96. PECs were pulsed with a dose range of mouse tissue–derived gp96. Cells were harvested after 4 h, lysed, and probed by immunoblotting with Abs specific to pro–IL-1β or actin as a loading control. The lower threshold of gp96 for induction of pro–IL-1β was between 0.1 and 1 μg/ml, reaching maximal induction at 10 μg/ml (Fig. 1A) (there is no statistical difference between 10 and 200 μg/ml). With 10 or 200 μg/ml gp96, pro–IL-β induction peaked at 4 h following stimulation with gp96 (Fig. 1B, Supplemental Fig. 1A). We postulated that the taper after 4 h was, in part, due to conversion of pro–IL-1β into IL-1β; upon which, recognition by the pro–IL-1β–specific immunoblotting Ab is lost. Alternatively, this could be due to the IL-10–driven negative feedback loop that shuts down the pro–IL-1β transcription induced by inflammatory signals (13). We used LPS, a known stimulator of pro–IL-1β, as a positive control (8). Pro–IL-1β induction with LPS peaked later than with gp96, consistent with earlier observations on kinetics of signaling induced by the two molecules (1, 2). Signaling via CD91, induced with gp96, is known to activate NF-κB and p38 MAPK (1), and we tested their role in the induction of pro–IL-1β. PECs were incubated with gp96 in the presence or absence of cardamonin or SB203580, inhibitors of NF-κB or p38 MAPK, respectively (1, 14). Pro–IL-1β was measured by immunoblotting. Pro–IL-1β induction was significantly impaired with either inhibitor (Fig. 1C, Supplemental Fig. 1B). Similar results were obtained with DCs (Supplemental Fig. 1C). To confirm CD91 dependency and, importantly, to eliminate the possibility that these observations were due to hypothetical contaminating endotoxin in the gp96 preparations, we harvested DCs from our novel $CD91^{fl/fl}CD11c^{Cre}$ mice (10) and tested pro–IL-1β synthesis. We show that in the absence of CD91 ($CD91^{fl/fl}CD11c^{Cre}$), APCs are unable to synthesize pro–IL-1β when stimulated with gp96 (Fig. 1D). As expected, these APCs make pro–IL-1β in response to LPS regardless of CD91 expression, consistent with a TLR2/4-dependent mechanism (15). These results are fully consistent with CD91-dependent IL-1β production observed previously (10). To test the induction of pro–Il-1β in vivo, we used an implantable cellular gp96-secretory system (16). In this study, B16 tumor cells express a gp96–Ig fusion construct (B16/gp96); 1×10^6 cells secrete ~300 ng of gp96 in 24 h (16). B16/gp96 or parental B16 cells (with empty vector) were implanted into the peritoneal cavity of mice, targeting the same PECs we used in vitro. At 8 or 18 h posttumor implantation, we analyzed pro–IL-1β in $F4/80^+CD91^+$ cells by flow cytometry (Supplemental Fig. 1D). Significant amounts of pro–IL-1β were produced at 8 h when B16/gp96 cells were implanted, but not B16 cells (Fig. 1E, 1F). Pro–IL-1β converted to mature IL-1β at 18 h (Fig. 1F). Next, we confirmed that pro–IL-1β was being made by macrophages (20% of total cells), which are the $CD91^+$ cells in the peritoneal cavity using the Amnis ImageStream. We show that 4.8% of total cells are $CD91^+$ and are synthesizing pro–IL-1β (Fig. 1G, Supplemental Fig. 1E). Importantly, no neutrophils (0.0% of $Ly\text{-}6G^+$) make IL-1β.

Macrophages release IL-1β in response to extracellular gp96 in vivo

We examined the release of IL-1β by PECs in response to gp96, following production of pro–IL-1β. PECs were stimulated with 10 or 200 μg/ml gp96 (doses of gp96 at which peak pro–IL-1β was produced) for 0–20 h. IL-1β was measured by ELISA. PECs were observed to continually release IL-1β in response to gp96 (Fig. 2A). Release of IL-1β was titratable with dose of gp96. We used our cellular, gp96-secretory system in this study to examine IL-1β production

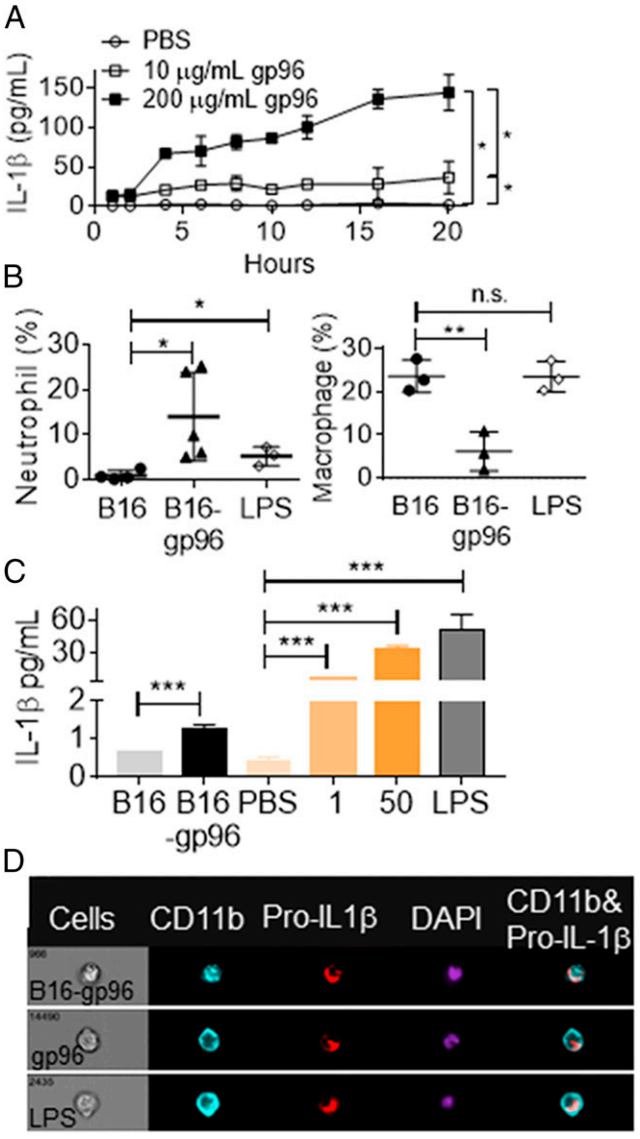

FIGURE 2. Macrophages release IL-1β in response to extracellular gp96 in vivo. (**A**) PECs were treated with different doses of gp96 or PBS in vitro. Supernatants of the culture were harvested at indicated time points, and IL-1β was measured by ELISA. (**B**) Macrophage ($F4/80^+Ly\text{-}6G^-$) and neutrophil ($F4/80^-Ly\text{-}6G^+$) populations in peritoneal cavity of mice were analyzed by flow cytometry 18 h after implantation of B16 or B16/gp96 or injection of 20 μg LPS. (**C**) Blood was collected from mice 8 h after i.p. injection of PBS, B16, B16/gp96, or gp96 at the indicated dose or LPS. IL-1β in serum was measured. (**D**) B16/gp96 (2×10^6), gp96 (50 μg), or LPS (20 μg) were injected i.p., and cells were analyzed 8 h later for intracellular pro–IL-1β in $CD11b^+$ cells. $^*p < 0.05$, $^{**}p < 0.01$, $^{***}p < 0.001$.

in vivo. The extravasation of neutrophils into the peritoneal cavity is dependent on IL-1β (17). We examined changes in immune infiltrate in response to extracellular gp96. Gp96, secreted by B16/gp96 cells, induced the extravasation of neutrophils into the peritoneal cavity 18 h after transplantation (Fig. 2B, Supplemental Fig. 1G). The increase in neutrophils was not observed when control B16 cells were introduced, suggesting the observed neutrophil extravasation was a gp96-mediated event rather than related to implantation of cells (Fig. 2B). The increase in the percentage of neutrophils (2–25%) corresponded to a similar reduction in the percentage of macrophages. Introduction of the bacterial product LPS caused some changes in neutrophil, but not macrophage, populations at 18 h, which is consistent with previous reports (17). This provides a contrast in the cellular dynamics and kinetics of inflammation induced with gp96 versus LPS (Fig. 2B). Next, we directly measured IL-1β in the blood following extracellular localization of gp96, either secreted from cells or via i.p. injection. Mice were implanted with B16 or B16/gp96 or injected with PBS, gp96, or LPS. IL-1β was measured in serum 8 h later (Fig. 2C). The gp96 produced by B16/gp96 in this time was ~200 ng. Serum IL-1β was detected when B16/gp96 was implanted, but not B16. Serum IL-1β was titratable with the dose of gp96 injected (Fig. 2C). We compared gp96 secreted from B16/gp96 cells with purified gp96 introduced via i.p. injection to confirm the cellular source of IL-1β. PECs were harvested after 8 h and analyzed with the Amnis ImageStream. Regardless of the source of gp96, pro–IL-1β was produced by $CD11b^+$ macrophages (3–9% of total cells). LPS also induced pro–IL-1β in macrophages (5% of total cells) as expected (Fig. 2D, Supplemental Fig. 1F).

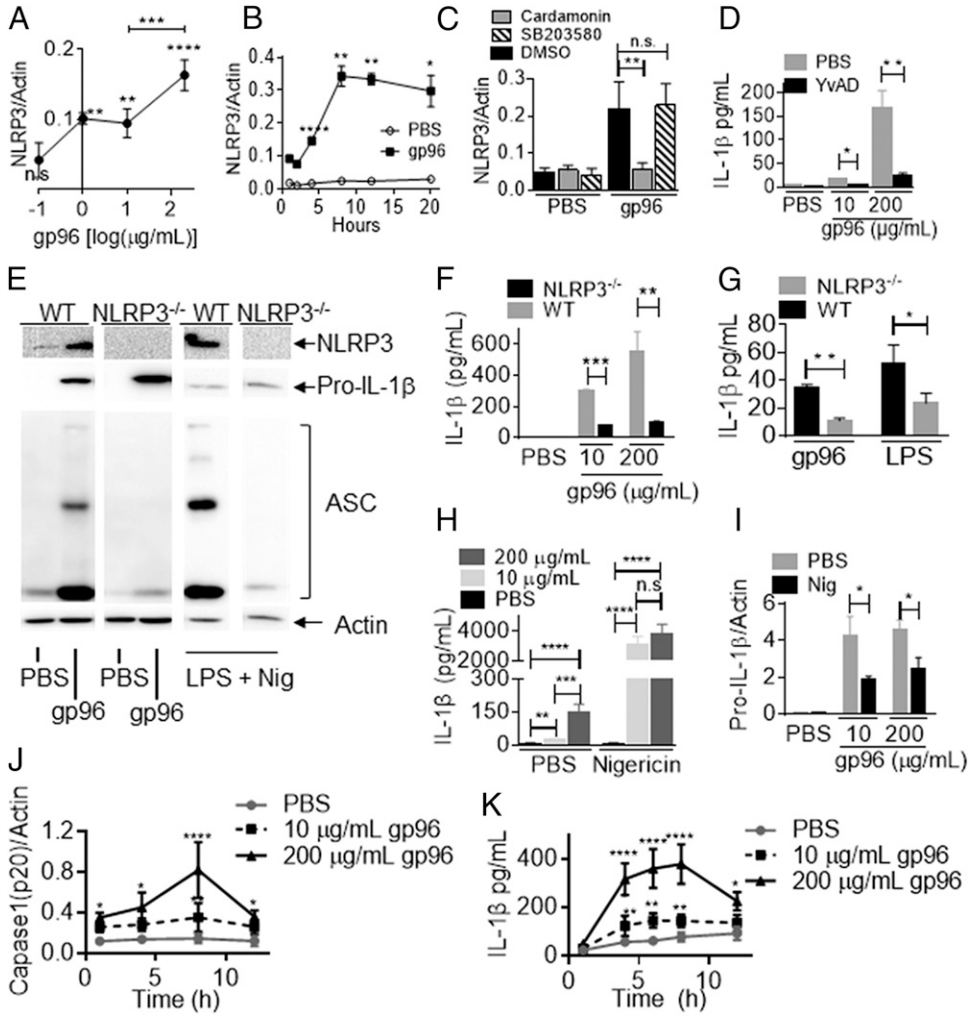

FIGURE 3. Gp96 activates inflammasomes for IL-1β release. (**A** and **B**) PECs were treated with PBS or gp96 at the indicated concentrations for 4 h (A) or over time (B). NLRP3 was analyzed by SDS-PAGE and immunoblotting. (**C**) PECs were treated with cardamonin or SB203580, followed by incubation with 200 μg/ml gp96 or DMSO. NLRP3 was analyzed as in (A). (**D**) PECs were treated with YVAD, followed by incubation with gp96 or PBS. IL-1β was measured as in (A) after 4 h. (**E** and **F**) PECs were harvested from WT or $NLRP3^{-/-}$ mice and treated with 10 (F) or 200 μg/ml (E and F) gp96 or PBS for 4 h. (E) NLRP3 or pro–IL-1β and ASC oligomerization were analyzed as in (A). PECs treated with a combination of LPS and nigericin as a positive control (E). IL-1β was measured by ELISA (F). (**G**) Blood was collected from WT or $NLRP3^{-/-}$ mice 8 h after i.p. injection of gp96 (50 μg) or LPS (20 μg). IL-1β was measured in the serum by ELISA. (**H** and **I**) PECs were treated with gp96 at the indicated dose or PBS for 4 h. The treated PECs were incubated for a further 30 min with nigericin or PBS. IL-1β was measured in the culture supernatant (H), whereas cell lysates (I) were harvested and analyzed as in (A). (**J** and **K**) PECs were primed with 300 ng/ml LPS for 3 h and then activated with gp96 for different times. (J) Cell lysate was collected, and cleaved caspase-1 (p20) was analyzed by immunoblotting. (K) IL-1β concentration in supernatants was tested by ELISA. In panels (A), (B), (G), and (I), the amount of pro–IL-1β or NLRP3 or caspase-1 was quantified and normalized to actin as a loading control. In (A) and (B), comparisons are made to PBS-treated cells. Data are from one representative experiment of three to five independent experiments. $^*p < 0.05$, $^{**}p < 0.01$, $^{***}p < 0.001$, $^{****}p < 0.0001$

Gp96 simultaneously upregulates pro–IL-1β and components of NLRP3 inflammasome

The main mechanism for conversion of pro–IL-1β to the mature IL-1β requires inflammasome activation. In preparation for such activation, expression of various constituent proteins are upregulated. We measured NLRP3 levels following treatment of cells with gp96. PECs were incubated with titrated doses of gp96 for 4 h. Cells were lysed and probed by immunoblotting for NLRP3. Induction of NLRP3 was observed with 1 μg/ml gp96, increasing with gp96 to 200 μg/ml (Fig. 3A, Supplemental Fig. 1H). The levels of NLRP3 were sustained and stable for over 20 h following stimulation with gp96 (Fig. 3B, Supplemental Fig. 1I), consistent with its observed half-life in cells (18). We next tested whether the induction of NLRP3 was dependent on NF-κB and p38 MAPK. PECs were treated with gp96 in the presence or absence of cardamonin or SB203580. In Fig. 3C and Supplemental Fig. 1J, we show that NLRP3 induction by gp96 was dependent on NF-κB, but not p38 MAPK. These signaling pathways are consistent with earlier observations (1, 6).

Release of IL-1β in response to gp96 is inflammasome dependent

We next tested the involvement of inflammasome constituents in gp96-mediated IL-1β release. PECs were treated with the caspase-1 inhibitor YVAD prior to, and for the duration of, gp96 stimulation. YVAD was observed to inhibit the IL-1β released in response to gp96 (Fig. 3D). We used the FAM-YVAD-FMK fluorescent inhibitor probe to label active caspase-1 enzyme in responding cells. A significant number of macrophages responded to titratable amounts of gp96 by activating caspase-1 (Supplemental Fig. 2A). Oligomerization of the adaptor protein ASC is a key indicator of inflammasome activation (19). ASC oligomers were observed in PECs stimulated with gp96 for 4 h (Fig. 3E). In the absence of the sensor protein NLRP3 (in PECs from NLRP3$^{-/-}$ mice), no ASC oligomerization was observed. As a positive control, robust ASC oligomerization was observed when WT, but not NLRP3$^{-/-}$ cells, were stimulated with 10 μg/ml LPS plus 10 μM of the synthetic antibiotic nigericin, known stimulators of the inflammasome in macrophages (12) (Fig. 3E). We next stimulated PECs from NLRP3$^{-/-}$ or WT mice with gp96. IL-1β release by NLRP3$^{-/-}$ PECs in response to gp96 was severely attenuated (Fig. 3F). We also tested whether serum IL-1β, observed in response to injected gp96, was inflammasome dependent. WT or NLRP3$^{-/-}$ mice were injected with gp96 (50 μg) or LPS (20 μg). Serum IL-1β was measured by ELISA (Fig. 3G). Results show that there is a significant decline in IL-1β in the serum in the absence of NLRP3. We compared the relative extent of inflammasome activation by gp96, an endogenous protein, with nigericin, which acts as a K^+ ionophore (12). PECs were stimulated with gp96 for 4 h, followed by a 30-min pulse with nigericin. Nigericin overwhelmingly boosted the release of IL-1β compared with PECs stimulated with gp96 alone (Fig. 3H). The increased release of IL-1β induced by gp96 plus nigericin led to a corresponding decrease in the inflammasome substrate pro–IL-1β (Fig. 3I, Supplemental Fig. 2B). To confirm that gp96 could activate inflammasomes, cells were primed with LPS for 3 h and then stimulated with gp96 over a timecourse. Cells treated with this regimen activated caspase-1 (Fig. 3J, Supplemental Fig. 2C) and released IL-1β (Fig. 3K).

Inflammasome activation by gp96 requires K^+ efflux, but not ROS production or P_2X_7

To understand how gp96 was activating the inflammasome, we stimulated PECs with gp96 in the presence or absence of inhibitors to K^+ efflux, ROS, and P_2X_7. IL-1β production was measured after 4 h. KCl in the medium, which inhibits K^+ efflux from cells, abrogated the production of IL-1β induced by gp96 by inhibiting inflammasomes as measured by caspase-1 activation (Fig. 4A, 4B). At the same molarity, NaCl had no effect on IL-1β production induced by gp96. However, inhibition of ROS production with *N*-acetylcysteine (Fig. 4C) or blocking the ATP receptor P_2X_7 with A438079, which is one way of mediating K^+ efflux after extracellular ATP binding, had no effect on IL-1β production (Fig. 4D). Interestingly, CD91 was recently shown to directly associate with Ca^{2+}-activated K^+ channels and modulate this channel to the open state upon binding to one of its non-HSP ligands, α2-macroglobulin (20). This could provide a direct mechanism through which CD91 drives a decline in intracellular K^+ concentrations, thereby activating inflammasomes. This is consistent with our observation that activation of

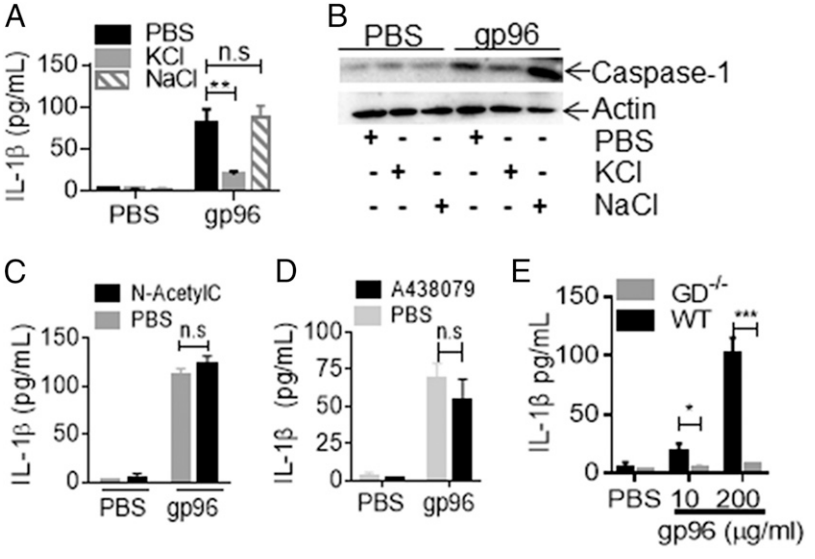

FIGURE 4. Gp96 activates inflammasome via K^+ efflux. (**A**–**D**) PECs were treated with 200 μg/ml gp96 or PBS in the presence or absence of (A and B) 20 mM KCl or NaCl, (C) 2 mM *N*-acetylcysteine, or (D) 25 μM A438079. IL-1β in culture supernatants was measured (A, C, and D), and cell lysates were harvested and analyzed for caspase-1 (p20) by SDS-PAGE and immunoblotting (B) after 4 h. (**E**) WT or GD$^{-/-}$ PECs were treated with PBS or gp96 for 4 h. IL-1β concentration in supernatant was measured by ELISA. Data are from one representative experiment of three to five independent experiments. $^*p < 0.05$, $^{**}p < 0.01$, $^{***}p < 0.001$.

inflammasomes by gp96 is dependent on cellular K^+ efflux. Another damage-associated molecular pattern (DAMP), ATP, acts through its own receptor P_2X_7 to also modulate K^+ channels (21). There are notable differences in the kinetics of NLRP3 inflammasome activation by gp96 and these other DAMPs, which may be physiologically relevant. The activation by gp96 could indicate that the kinetics of K^+ efflux induced by gp96 are slow and require chronic exposure of APCs to this signal compared with the immediate K^+ efflux induced by ATP or nigericin. Alternatively, gp96 could activate the NLRP3 inflammasomes indirectly, requiring other endogenous signals.

The evolution of inflammasomes as an important detection and response mediator to infection has been well characterized (8). We show in this study that the release of IL-1β in response to extracellular gp96 is dependent on NLRP3 inflammasomes. In contrast to other activators of the inflammasomes, gp96 also upregulates the inflammasome substrate pro–IL-1β and components for the inflammasome NLRP3. Thus, gp96 as a single entity simultaneously provides signals for both arms necessary for IL-1β release. Multiple immunogenic HSPs, including hsp90, hsp70, and calreticulin, engage CD91 and cause the release of IL-1β from APCs in vitro without additional stimuli (1). Activation of inflammasomes by these HSPs remains to be formally tested. Different inflammasome sensors may be involved with these HSPs following other DAMPs, like dsDNA, which use AIM2 inflammasomes (22). Robust inflammasome activation and activity is typically associated with some cell death, including pyroptosis (8, 22). We show that gp96 triggered some cell death, measured by annexin V/propidium iodide positivity (Supplemental Fig. 2D), when compared with cell death induced by LPS/nigericin. Cell death and IL-1β release was GD-dependent (Fig. 4E, Supplemental Fig. 2D). Cell death was also induced in a GD-dependent manner when cells were primed by LPS and stimulated with 200 μg/ml gp96 (Supplemental Fig. 2E). Interestingly, IL-1β released under these conditions appeared not to rely on GD (Supplemental Fig. 2F), possibly because of alternative release mechanisms triggered by LPS stimulation and/or extended incubation times of this singular assay. We show that extracellular gp96 released by cells in vivo leads to plasma IL-1β and neutrophil extravasation. TNF-α, another cytokine required for extravasation, is also released from APCs stimulated with gp96 (1, 2). It is conceivable that the HSP-mediated activation of inflammasomes may be superseded or complemented during infection by stronger pathogen-associated molecular pattern–mediated activation of inflammation; however, they nonetheless are likely to contribute to the overall inflammatory picture. Sterile or tissue damage–associated inflammation has long been associated with various DAMPs. HSPs, the first DAMP, to our knowledge, to be identified (23), are abundant intracellular proteins, making their recognition by the immune system a strong surrogate for detection of cellular aberrancy in infectious and noninfectious conditions. Our studies suggest novel therapies targeting CD91 would be expected to be more effective at reducing inflammation than current inhibitors such as MCC950 targeting NLRP3, because CD91 is upstream of the inflammasomes and prior to signal amplification.

Acknowledgments

B16/gp96 was a kind gift from Dr. Eckhard Podack (University of Miami, FL). We thank Dr. Jia Xue for mouse tissues and Qian Sun and Chenxuan Yang for assistance with NLRP3$^{-/-}$ and GD$^{-/-}$ mice.

Disclosures

The authors have no financial conflicts of interest.

References

1. Pawaria, S., and R. J. Binder. 2011. CD91-dependent programming of T-helper cell responses following heat shock protein immunization. *Nat. Commun.* 2: 521.
2. Basu, S., R. J. Binder, R. Suto, K. M. Anderson, and P. K. Srivastava. 2000. Necrotic but not apoptotic cell death releases heat shock proteins, which deliver a partial maturation signal to dendritic cells and activate the NF-kappa B pathway. *Int. Immunol.* 12: 1539–1546.
3. Binder, R. J. 2014. Functions of heat shock proteins in pathways of the innate and adaptive immune system. *J. Immunol.* 193: 5765–5771.
4. Binder, R. J. 2008. Heat-shock protein-based vaccines for cancer and infectious disease. *Expert Rev. Vaccines* 7: 383–393.
5. Messmer, M. N., J. Pasmowitz, L. E. Kropp, S. C. Watkins, and R. J. Binder. 2013. Identification of the cellular sentinels for native immunogenic heat shock proteins in vivo. *J. Immunol.* 191: 4456–4465.
6. Kinner-Bibeau, L. B., A. L. Sedlacek, M. N. Messmer, S. C. Watkins, and R. J. Binder. 2017. HSPs drive dichotomous T-cell immune responses via DNA methylome remodelling in antigen presenting cells. *Nat. Commun.* 8: 15648.
7. Chandawarkar, R. Y., M. S. Wagh, and P. K. Srivastava. 1999. The dual nature of specific immunological activity of tumor-derived gp96 preparations. *J. Exp. Med.* 189: 1437–1442.
8. Davis, B. K., H. Wen, and J. P.-Y. Ting. 2011. The inflammasome NLRs in immunity, inflammation, and associated diseases. *Annu. Rev. Immunol.* 29: 707–735.
9. Afonina, I. S., C. Müller, S. J. Martin, and R. Beyaert. 2015. Proteolytic processing of interleukin-1 family cytokines: variations on a common theme. *Immunity* 42: 991–1004.
10. Zhou, Y. J., M. N. Messmer, and R. J. Binder. 2014. Establishment of tumor-associated immunity requires interaction of heat shock proteins with CD91. *Cancer Immunol. Res.* 2: 217–228.
11. Kayagaki, N., I. B. Stowe, B. L. Lee, K. O'Rourke, K. Anderson, S. Warming, T. Cuellar, B. Haley, M. Roose-Girma, Q. T. Phung, et al. 2015. Caspase-11 cleaves gasdermin D for non-canonical inflammasome signalling. *Nature* 526: 666–671.
12. Katsnelson, M. A., L. G. Rucker, H. M. Russo, and G. R. Dubyak. 2015. K+ efflux agonists induce NLRP3 inflammasome activation independently of Ca2+ signaling. *J. Immunol.* 194: 3937–3952.
13. Gurung, P., B. Li, R. K. Subbarao Malireddi, M. Lamkanfi, T. L. Geiger, and T. D. Kanneganti. 2015. Chronic TLR stimulation controls NLRP3 inflammasome activation through IL-10 mediated regulation of NLRP3 expression and caspase-8 activation. *Sci. Rep.* 5: 14488.
14. Cuenda, A., J. Rouse, Y. N. Doza, R. Meier, P. Cohen, T. F. Gallagher, P. R. Young, and J. C. Lee. 1995. SB 203580 is a specific inhibitor of a MAP kinase homologue which is stimulated by cellular stresses and interleukin-1. *FEBS Lett.* 364: 229–233.
15. Poltorak, A., X. He, I. Smirnova, M. Y. Liu, C. Van Huffel, X. Du, D. Birdwell, E. Alejos, M. Silva, C. Galanos, et al. 1998. Defective LPS signaling in C3H/HeJ and C57BL/10ScCr mice: mutations in Tlr4 gene. *Science* 282: 2085–2088.
16. Yamazaki, K., T. Nguyen, and E. R. Podack. 1999. Cutting edge: tumor secreted heat shock-fusion protein elicits CD8 cells for rejection. *J. Immunol.* 163: 5178–5182.
17. Ip, W. K., and R. Medzhitov. 2015. Macrophages monitor tissue osmolarity and induce inflammatory response through NLRP3 and NLRC4 inflammasome activation. *Nat. Commun.* 6: 6931.
18. Han, S., T. B. Lear, J. A. Jerome, S. Rajbhandari, C. A. Snavely, D. L. Gulick, K. F. Gibson, C. Zou, B. B. Chen, and R. K. Mallampalli. 2015. Lipopolysaccharide primes the NALP3 inflammasome by inhibiting its ubiquitination and degradation mediated by the SCFFBXL2 E3 ligase. *J. Biol. Chem.* 290: 18124–18133.
19. Lu, A., V. G. Magupalli, J. Ruan, Q. Yin, M. K. Atianand, M. R. Vos, G. F. Schröder, K. A. Fitzgerald, H. Wu, and E. H. Egelman. 2014. Unified polymerization mechanism for the assembly of ASC-dependent inflammasomes. *Cell* 156: 1193–1206.
20. Wakle-Prabagaran, M., R. A. Lorca, X. Ma, S. J. Stamnes, C. Amazu, J. J. Hsiao, C. M. Karch, K. L. Hyrc, M. E. Wright, and S. K. England. 2016. BKCa channel regulates calcium oscillations induced by alpha-2-macroglobulin in human myometrial smooth muscle cells. *Proc. Natl. Acad. Sci. USA* 113: E2335–E2344.
21. Mariathasan, S., D. S. Weiss, K. Newton, J. McBride, K. O'Rourke, M. Roose-Girma, W. P. Lee, Y. Weinrauch, D. M. Monack, and V. M. Dixit. 2006. Cryopyrin activates the inflammasome in response to toxins and ATP. *Nature* 440: 228–232.
22. Fernandes-Alnemri, T., J.-W. Yu, P. Datta, J. Wu, and E. S. Alnemri. 2009. AIM2 activates the inflammasome and cell death in response to cytoplasmic DNA. *Nature* 458: 509–513.
23. Srivastava, P. K., A. B. DeLeo, and L. J. Old. 1986. Tumor rejection antigens of chemically induced sarcomas of inbred mice. *Proc. Natl. Acad. Sci. USA* 83: 3407–3411.